7. A. V. Gurevich and L. P. Pitaevskii, "Recombination coefficient in a dense low-temperature plasma," Zh. Eksp. Teor. Fiz., 46, No. 4 (1964).
8. Ya. B. Zel'dovich and Yu. P. Raizer, Physics of Shock Waves and High-Temperature Hydrodynamic Phenomena [in Russian], Nauka, Moscow (1966).
9. M. P. Chaika and É. E. Fradkin, "Method for transforming spectral line contours and its application to measuring the temperature and other parameters of a light source," Opt. Spektrosk., 7, No. 9 (1959).
10. H. R. Griem, Plasma Spectroscopy, McGraw-Hill, New York (1964).
11. V. Vize, "Width of spectral lines," in: Plasma Diagnostics [Russian translation], Mir, Moscow (1967).

EXPERIMENTAL INVESTIGATION OF INTERACTION OF A SHOCK WAVE WITH A WALL CAVITY

E. F. Zhigalko, L. L. Kolyshkina, and V. D. Shevtsov

UDC 533.601.1

In unsteady gas flow one often meets the situation where a shock wave passes a location where the channel section changes. At a very early stage of the phenomenon, when there is no appreciable interference by structural elements, it is profitable to examine the phenomenon as a combination of elementary characteristic model problems in shock-wave–wall interaction. At a later stage it is often possible to use a one-dimensional approach and employ solutions of the discontinuity decay problem [1-3]. The investigation of the intermediate stage in this paper is based on experiments conducted in an air shock tube of rectangular section 130 × 80 mm whose channel overlaps a rigid wall normal to the tube axis, with a straight cavity of finite length. The examination concentrates on questions not inherently associated with the finite nature of the channel section ahead of the model.

The unsteady process examined here can be arbitrarily divided into phases, in accordance, for example, with changes in the wave configurations in each phase.

While the incident wave is penetrating the cavity, the gas, compressed behind the shock wave reflected from the forward sections of the wall, is flowing into the cavity, where the pressure is lower. The diffracted waves from the opposite edges repeatedly interact with each other and with the obstacle, thus modulating both the reflected wave and the wave penetrating the cavity.

Until one has a wave going through the channel its base pressure has the property of similarity for channels of different width H. The similarity does not extend to elements of the phenomenon which are intrinsically connected with the influence of dissipation, e.g., to the separation accompanying gas flow over the forward edges of the cavity. The sequence of vortices formed here is carried by the flow into the cavity, generating two systems of vortices about its walls, like Kármán streets, clearly visible on shadowgraph and interferometry pictures (Fig. 1a).

With the onset of the next phase when the wave in the cavity reaches the floor and reflects from it, the channel length L is added to the parameters of the problem. In modeling this and subsequent phases one can use only results consonant with similarity of flows about cavities of the same L/H ratio. One can consider, arbitrarily, that the second phase lasts until the shock wave reflected from the floor exits from the channel and the rarefaction wave penetrates into it.

Figure 2 (H = 10 mm) shows typical oscillograms obtained in calibrating a piezometric pressure sensor in a shock tube with the end closed (Fig. 2a, M = 1, 2), and in measurement of the pressure at characteristic points on the model: on the floor (Fig. 2b, M = 1.44) and at the forward edge (Fig. 2c, M = 1.24). Some of the sensor parameters are: sensitive element diameter 1.5 mm, maximum body diameter 6 mm, estimated self-frequency no lower than 100 kHz.

Leningrad. Translated from Zhurnal Prikladnoi Mekhaniki i Tekhnicheskoi Fiziki, No. 6, pp. 23-28, November-December, 1981. Original article submitted March 17, 1980.

 0021-8944/81/2206-0750$07.50 © 1982 Plenum Publishing Corporation

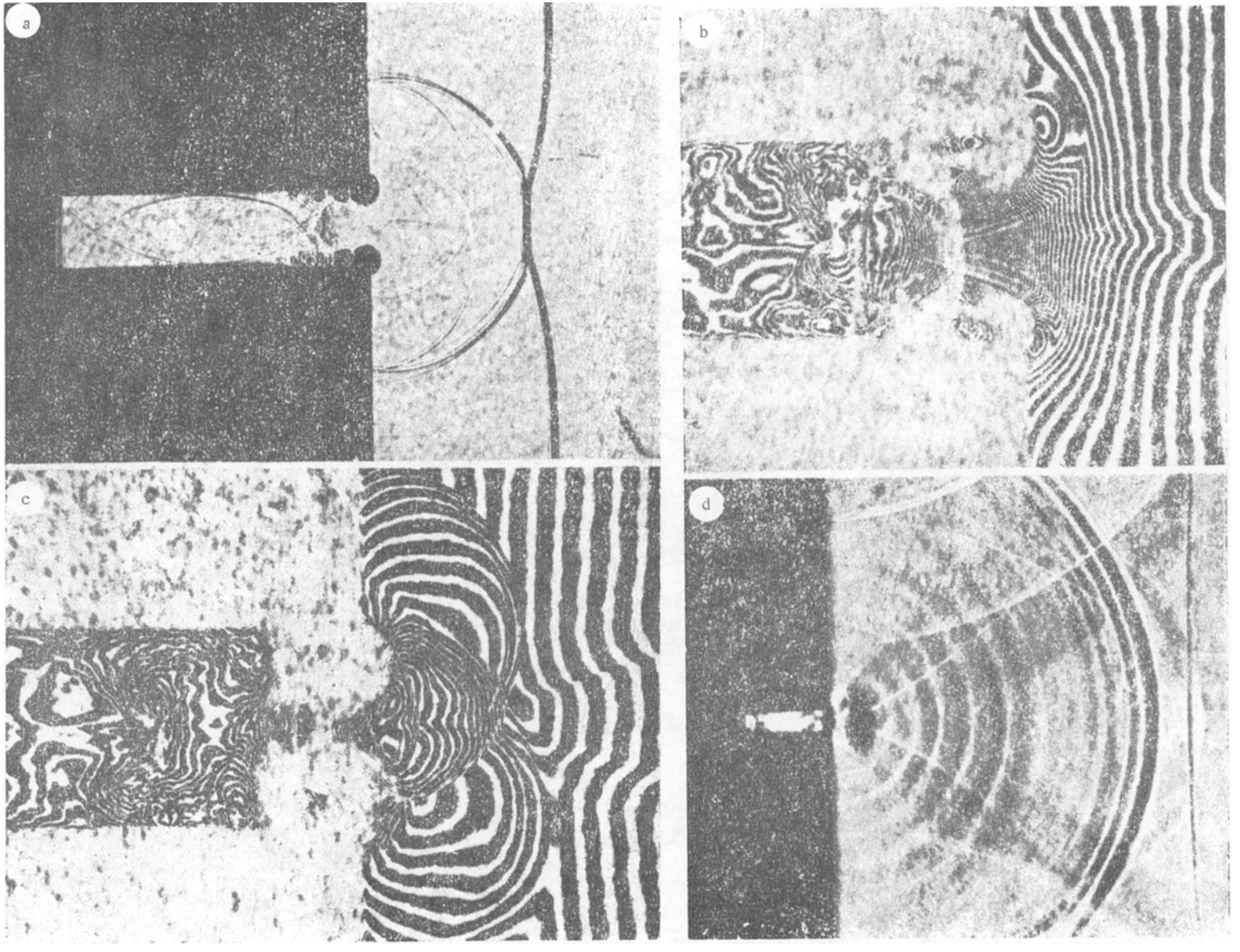

Fig. 1

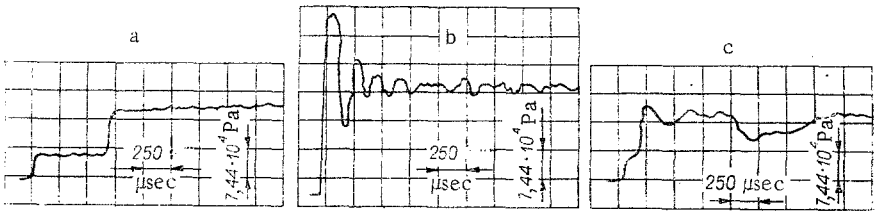

Fig. 2

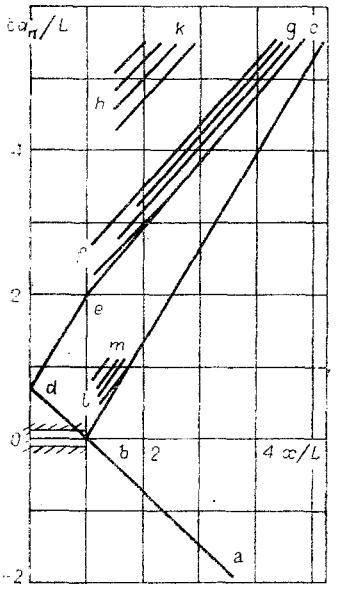

Fig. 3

High-speed photographs of the process obtained with a high-speed camera (SFR) give a clear picture of the course of the development. When processed these yield wave diagrams of the type of Fig. 3 (M = 1.535, ab is the incident wave, bc is the reflected wave, bd is the wave penetrating the cavity, de is the wave reflected from the rear wall of the cavity, lm is the first wave train, fg is the second wave train, hk is the third wave train).

Extensive information on the phenomenon is given by the shadowgraph and interferometric photographs of the flow field, obtained with the help of an IAB-451 shadowgraph instrument, equipped with a laser and an interference attachment [4]. Examples of this kind of picture, corresponding to different phases of the process, are given in Fig. 1 (an air shock tube of rectangular section 130 × 80 mm; cavity width in Fig. 1a-c is 10 mm, and in Fig. 1d it is 5 mm). The additional use of colored shadowgraph pictures obtained by reconstructing the wave front from individual holograms [5] facilitated the analysis of the phenomenon and enriched the results.

In the experiments we used models with a cavity of L/H = 4.

In examining the readings of the pressure sensors (Fig. 2b, c), and also the results of optical observation of the flow field (Fig. 1a-d), one can form the conclusion that several regular wave systems are present typically in the process studied. After the shock wave strikes the obstacle there is shock excitation of the cavity. Like an oscillator it emits a system of waves whose length is correlated with L. These waves are modulated in amplitude, since the effects at the forward edges generate higher frequency oscillations (of length $\sim$H).

We now consider the conditions for generating the first wave packet. It was noted above, in discussing the first phase of the phenomenon, that the diffracted reflected shock wave in the channel proper near the start of the cavity edge moves to the opposite wall of the cavity. On the way it meets the wave moving from the opposite edge. In turn, the shock waves (the product of the interaction), arriving at the cavity edge, undergo a reflection there, and with the reflected waves the above process of transverse motion at the cavity mouth is repeated many times. Each time, as the shock wave reaches the cavity edge a

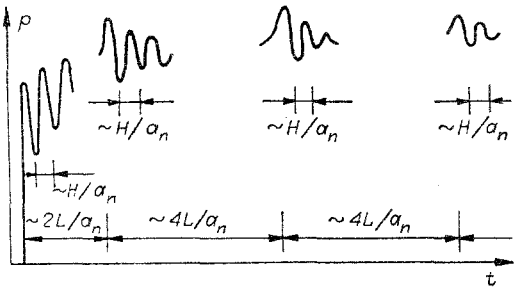

Fig. 4

cylindrical reflected shock wave is radiated. The waves radiated simultaneously at the opposite edges interfere, and at a certain distance from the cavity mouth only the resultant wave is distinguishable. The packet of weak shock waves thus radiated moves ahead of the originally reflected shock, which also weakens the wave train. Since the conditions behind the reflected shock wave are close to those given by the normal shock parameters, while the waves at the cavity mouth are weak, the result is that each successive wave train is radiated after an interval $\sim H/a_n$. Therefore, they should be separated from each other by a distance $\sim H$ on a photograph of the wave train. This can be confirmed by the Fig. 1a example.

The conditions for generating the second and subsequent trains differ from the process described above. The second train is radiated after the time interval required for the shock wave in the cavity to travel the distance from the cavity mouth to the floor and back. In the experimental conditions the pair of very strong vortices at the mouth, generated by the flow over the leading edges of gas directed into the cavity, determines the emergence of this wave from the cavity up to the time when the shock wave reflected from the floor approaches the cavity mouth. The vortices cover the central part of the channel, and the shock wave breaks through outside in a thin layer along the wall (Fig. 1b, c). At this time each edge radiates a cylindrical shock wave. When these unite at some distance from the cavity (Fig. 1c), they head up the second wave train, and when reflected from the opposite edges, and so on, excite the waves composing this train.

Subsequent wave packets are radiated after the time interval required for the motion: of the rarefaction wave from the mouth to the floor, of the reflected rarefaction wave from the floor to the mouth, of the compression wave from the mouth to the floor, and of the reflected compression wave from the floor to the mouth. An estimate of this interval is the time $4L/a_n$, i.e., it is appreciably larger than the time between radiation of the first and second wave packets ($\sim 2L/a_n$).

Thus, in radiating wave packets, the cavity acts like a Helmholtz resonator. The wave frequency in all the packets can be evaluated approximately by the quantity H/a_n.

The two wave systems radiated by the cavity are attenuated. The systems of radiated waves are shown schematically in Fig. 4. The first four trains can be seen in the experiments.

Figure 5 shows the distributions of density ρ, obtained by reducing the interferograms, referenced to the density under normal conditions ρ_0, along the flow symmetry axis for the second phase of the phenomenon, for a model with H = 10 mm and M = 1.34, t = 115 msec (curve 1), and M = 1.60, t = 89 msec (curve 2). The reflected wave is close in strength to the normally reflected value. Later the density falls off towards the mouth of the cavity. It reaches its least value at a section of the cavity located at a certain distance from the mouth ($x/L \sim 0.1$), due to separation processes at the leading edges and the reduction of the tube flux section here. Acceleration of the gas in this case can lead to supersonic flow and, as a result, to the appearance of a stagnation shock wave here. This wave is present in the results shown in Fig. 1a, b. Since it is a structure characteristic of the first phase of the phenomenon, the conditions for its occurrence do not depend on the channel geometry, and therefore are determined only by the Mach number of the incident wave. One can estimate these conditions crudely as follows. The processes at the cavity mouth are similar to a discharge under the action of the pressure drop $p_n - p_1$ (p_n, p_1 are the normally reflected pressure and the pressure behind the incident wave, respectively). This kind of discharge becomes supersonic for $p_n/p_1 \gtrsim 1.89$, which corresponds to $M \gtrsim 1.37$. It

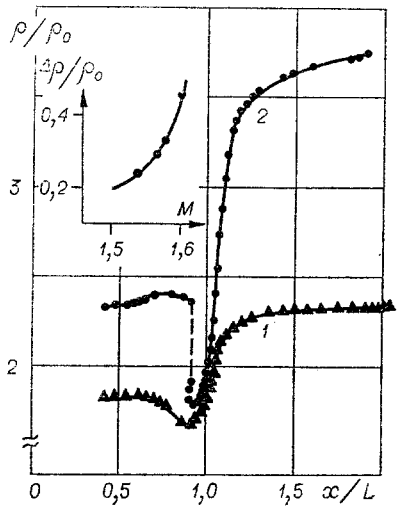

Fig. 5

should be noted that this estimate is confirmed in the experiments. A stagnation shock wave was observed only for M > 1.4. Figure 5 shows the measured density discontinuity on this wave, and in the upper left corner is given the measured amplitude of the stagnation discontinuity. Apropos of the reduction of the interferograms it should be noted that the transition through the shock was accomplished indirectly along the boundary layer.

LITERATURE CITED

1. V. G. Dulov, "Decay of the arbitrary breakdown of parameters of a gas at a discontinuity in the cross section," Vestn. Leningr. Gos. Univ., No. 19, 4 (1958).
2. I. K. Yashev, "Decay of arbitrary breakdown in a channel with a distontinuity in cross sectional area," Izv. Sib. Otd. Akad. Nauk SSSR, Ser. Tekh. Nauk, 2, No. 8 (1967).
3. R. F. Chisnell, "Motion of a shock wave in a channel, with applications to cylindrical and spherical shock waves," J. Fluid Mech., 2, 286 (1957).
4. V. A. Komissaruk, V. P. Martunov, and N. P. Mende, "The use of a diffraction interferometer in a ballistic experiment," Prib. Tekh. Eksp., No. 207 (1979).
5. I. S. Zeilikovich, V. A. Komissaruk, et al., "Some capabilities of shear interferometers when tuned to dense bands," Zh. Tekh. Fiz., 49, No. 3 (1979).